sustainability

MDPI

Article

Research on Drilling Response Characteristics of Two-Wing PDC Bit

Cancan Liu *, Xigui Zheng *, Gang Wang, Mengbin Xu and Zhishang Li

Key Laboratory of Deep Coal Resource Mining, Ministry of Education of China, School of Mines, China University of Mining & Technology, Xuzhou 221116, China; TS18020044A31@cumt.edu.cn (G.W.); TS18020054A31@cumt.edu.cn (M.X.); TS18020074A31@cumt.edu.cn (Z.L.)

* Correspondence: liucancan@cumt.edu.cn (C.L.); 3774@cumt.edu.cn (X.Z.)

Received: 19 October 2019; Accepted: 1 January 2020; Published: 4 January 2020

check for updates

Abstract: Research on drilling response characteristics of two-wing polycrystalline diamond compact (PDC) bit in different rocks is an important way to further understand the mechanism of rock-breaking, improve drilling efficiency, and identify the rock formation interfaces in coal mines. However, the research on the drilling response characteristics of two-wing PDC bits is relatively rare due to the harsh environment in coal mines. In this study, a series of two-wing PDC bits were used to drill in sandstone and sandy mudstone to study the response characteristic of sound pressure level, displacement curves, longitudinal vibration, and rock cuttings size. The collected data were processed by MATLAB based on the 3σ principle. The cuttings were collected through a newly designed cuttings collection device. The experimental results show that the sound pressure level and the longitudinal vibration are larger when drilling in the higher strength sandstone, which is opposite to the cuttings particles and the penetration rate. The reduction of drilling efficiency is more obvious when drilling in sandstone with a worn bit. Therefore, drilling efficiency can be improved by optimizing the bit structure so that the broken rock blocks flow out of the anchor holes as early as possible to avoid being broken into cuttings.

Keywords: drilling efficiency; drilling response characteristics; PDC bit; rock cuttings

---

1. Introduction

Polycrystalline diamond compact (PDC) bits are widely used to drill various formations in oil and gas, mining engineering, and other fields. Consequently, it is crucial to study the rock-breaking mechanism of PDC bits. For example, quasi-static indentation and dynamic impact experiments were performed on sandstone, granite, and basalt to examine the interaction between bit and rock [1]. The rock-breaking mechanism of cross-cutting PDC bit was investigated by laboratory experiments and numerical simulation [2]. The rock-breaking mechanism under single-tooth impact was studied by theoretical derivation and numerical simulation [3]. In addition, several studies [4–6] have been conducted to understand the drilling response characteristics of wear PDC bits. For instance, the model based on the relationship between cutting and friction stress related to the drag bits excavation mechanism was implemented in order to evaluate cutting efficiency and to estimate wear of the diamond insert [4]. A close relationship between the bit wear condition and bit torque was found by drilling tests conducted in the laboratory using Percussion bits, PDC bits, roller cone bits, and various rocks [5]. The relationships between geometric patterns of carbide-tipped bit wear and rate of penetration were evaluated by drilling concrete in the laboratory [6]. However, the sound pressure level, longitudinal vibration, and cuttings particle characteristics of worn bits when drilling in rock formations of different strengths have not been properly studied yet. Additionally, rock-breaking processes and drill geometry have been studied by many researchers to improve drilling efficiency.

For example, rock fragmentation processes induced by double drill bits subjected to static and dynamic loading were examined by a numerical method [7]. The propagation of cracks and the characteristics of cuttings in the drilling process were investigated by using a high-speed camera in the laboratory [8,9]. Wang et al. (2018) discussed the influences of different bottom hole shapes on the effectiveness of rock-breaking [10]. Percussion drilling tests were carried out in a laboratory to evaluate the drilling performance of PDC percussion bits [11]. The directional drilling PDC bit used in coal mines was optimized by the numerical simulation method [12]. An annular-groove PDC bit was proposed to improve rock-breaking efficiency [13]. However, the rock-breaking efficiency of different bits in rock strata with different strengths has not been studied in depth. Rock formation identification based on PDC bit response characteristics is also a research hotspot. For instance, the penetration rate and vibration characteristics of two-wing PDC bits in rock strata with different strengths were studied to identify various rock interfaces [14]. Li's doctoral dissertation focuses on the identification of rock mass properties based on drilling response [15]. The vibration mechanism and characteristics of the drill pipe when drilling the bolt holes in the roof were analyzed by numerical simulations [16]. Noise characteristics of roller cone bit, diamond core bit, and PDC core bit were analyzed [17]. However, the sound pressure level, longitudinal vibration, and cuttings particle distribution characteristics of various two-wing PDC bits when drilling in rock strata of different strengths have not been comprehensively studied. Moreover, it has been found from the previous research, a large amount of work has been carried out to study the rock-breaking mechanism of PDC bit, shown in Figure 1. Conversely, the drilling characteristics of the two-wing PDC bit, shown in Figure 2, have not been extensively studied. In addition, the previous research work was mainly implemented through numerical simulations and laboratory experiments, which is also different from the actual situation on site. Therefore, in this paper, the drilling characteristics of two-wing PDC bits are analyzed to further understand the rock-breaking mechanism of two-wing PDC bit based on field experiments.

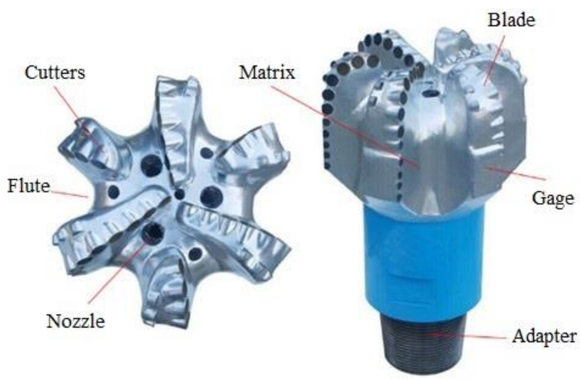

Figure 1. The structure of polycrystalline diamond compact (PDC) bit [18].

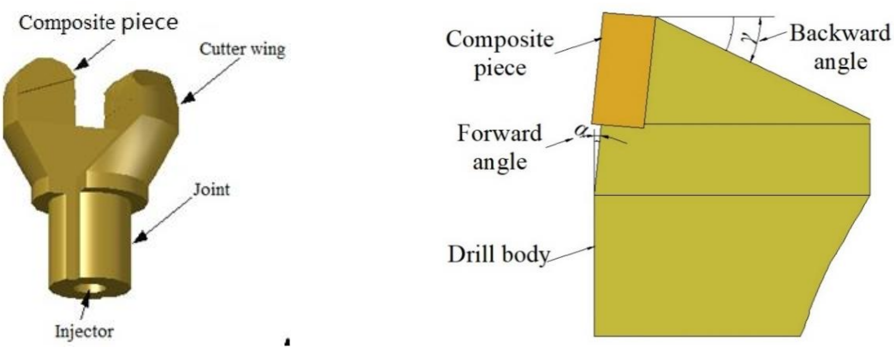

(**a**) 3D model established (**b**) Single cutting wing model

Figure 2. The structure model of the two-wing PDC bit.

2. Experimental Study

2.1. Experimental Apparatus

The schematic diagram of the experimental device is illustrated in Figure 3. The cuttings collection device, passed by a 19 mm diameter hexagonal prism drill pipe, consists of a 200 mm diameter cuttings funnel made of plastic and a 500 mL measuring cylinder. The angle between the cuttings funnel and the drill pipe is 30°, to facilitate, the person has to hold the measuring cylinder to collect the cuttings during the drilling process. The MQT-130/3.2 pneumatic anchor rig used for drilling has a rated output of 3.2 kW, a rated torque of 130 N·m, a rated speed of 240 rpm, and a working pressure of 0.4 to 0.6 MPa. The displacement sensor with a frequency of 25 Hz and an accuracy of ±1 mm was fixed on the leg of the anchor rig for collecting displacement data between the displacement sensor and ground during the drilling process and transmitted to the computer through a cable. The acoustic recorder connected to the computer has a sampling frequency of 1 Hz. The displacement sensor and acoustic recorder have correspondingly designed data acquisition software installed on the computer.

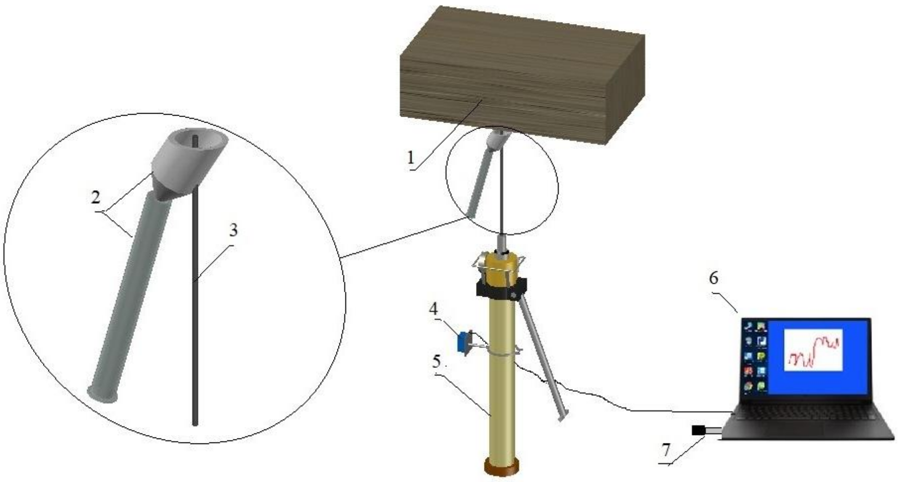

1—Roadway roof, 2—cuttings collection device, 3—drill pipe, 4—displacement sensor, 5—pneumatic anchor rig, 6—computer, 7—acoustic recorder

Figure 3. The picture of the experimental devices' connection.

2.2. Experimental Program

The experiment was divided into two groups, which were conducted in the 11074 return airway of Panzhihua Coal Mine and the P41106 transport roadway of Wangjiazhai Coal Mine in Guizhou Province, respectively. According to the geological data, the rock properties of the roadway roof in the experimental section are 7 m sandstone (Uniaxial Compressive Strength (UCS) is about 80 MPa) and 6.5 m sandy mudstone (UCS is about 35 MPa). The drill bits used in the experiments were manufactured by the corporation of Qidong County Front Speed Drilling Tool. The drill body and composite piece are made of 45# steel body and polycrystalline diamond respectively. The type of the connection thread and length are M14 × 1.5 and 20 mm respectively. The main information of the five drill bits used in the experiments is listed in Table 1.

Table 1. Basic information about the drill bits in the experiments.

Drill Bit Number	Type	Diameter/mm	Height/mm	α/(°)	γ/(°)	Weight/g
1	new	28	47.54	6	25	72
2	new	30	46.89	7	25	79
3	new	32	48.41	6	24	84
4	new	42	58.61	6	23	186
5	worn	28	35.83	5	9	52

It can be seen from the photograph shown in Figure 4, that the drill bit has been severely worn and its height and weight have been significantly reduced.

Figure 4. No. 5 worn bit.

According to the drilling arrangement shown in Figure 5, the five drill bits were used to drill in the sandy mudstone and sandstone roof. The drilling phase is divided into three sections [19]. To study the characteristics of the drilling stabilization phase, two black markers were used on the drill pipe at 5 cm and 15 cm, respectively. Displacement acquisition, sound pressure recording, and cuttings collection were carried out when the drilling depth was between 5 cm and 15 cm. In parallel, the supply pressure was required to be 0.5 ± 0.05 MPa during the drilling process, and the rig was not allowed to sway to ensure the same experimental conditions. Drilling experiments were carried out in the same way in the 11074 return airway of Panzhihua Mine.

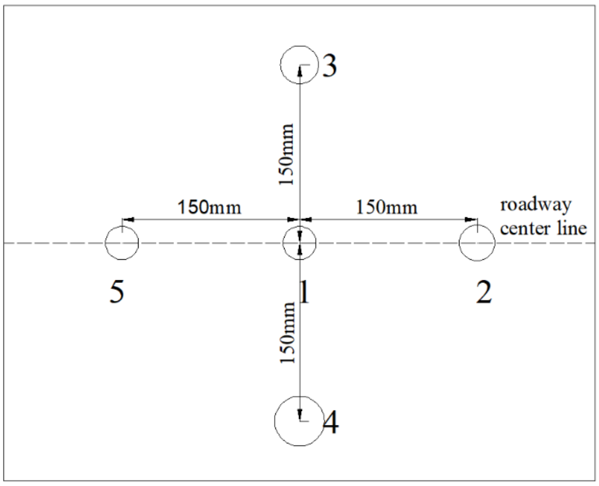

Figure 5. The layout of the experimental boreholes in the roof of the roadway. The boreholes number in the Figure corresponds to the drill bit number in Table 1.

2.3. The Rock Cuttings Screening Method for Different Particles

There are four sieves of 20 cm in diameter and 5 cm in height, and the diameters of these meshes are 0.8 mm, 0.5 mm, 0.28 mm, and 0.074 mm, respectively. These sieves are used to separate cuttings into different particle sizes.

Firstly, the cuttings collected for each hole was weighed by the electronic scale (Accuracy ±1 g) and recorded as M. Then, the quality of the cuttings was correspondingly recorded as m_1, m_2, m_3, and m_4, which are sequentially sieved with sieves having mesh diameters of 0.074 mm, 0.25 mm, 0.5 mm, and 0.8 mm. The corresponding relationship between the quality of different cuttings particles is shown in Table 2.

Table 2. Correspondence of different cuttings particle quality.

Borehole Number	0~0.074 mm	0.074~0.25 mm	0.25~0.5 mm	0.5~0.8 mm	>0.8 mm
1	M-m_1	M-m_1-m_2	M-m_1-m_2-m_3	M-m_1-m_2-m_3-m_4	m_4

2.4. Data Processing Method

There may be abnormal values in the data collected by the displacement sensor and the acoustic recorder. Here, the 3σ principle is used for abnormal values detection. The probability density of the 3σ principle sample data shown in Figure 6 means that the probability of the sample is 0.26% in the range of $(-\infty, \mu - 3\sigma)$ and $(\mu + 3\sigma, +\infty)$, which is called the anomaly point under the 3σ principle [20]. Obviously, the displacement data does not obey the positive distribution of mean μ and standard deviation σ. Assuming that under certain conditions, the penetration rate and sound pressure during drilling in the rock of the same strength obey the positive distribution. Consequently, the abnormal values of the corresponding displacement can be found by detecting the abnormal values of the penetration rate.

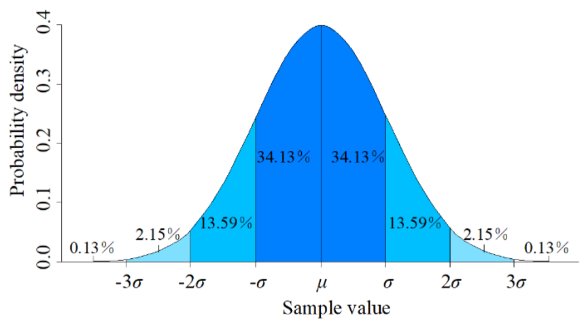

Figure 6. Schematic diagram of 3σ.

Assuming that the sample data acquired by the displacement sensor are (t_i, S_i) (I = 1, 2, 3, . . . , m), the penetration rate $V(t_i)$ can be expressed as Equation (1).

$$V(t_i) = \frac{S_i - S_{i-1}}{t_i - t_{i-1}}, (i = 2, 3, 4, \cdots, m) \tag{1}$$

where (t_i, S_i) indicates that the displacement at time t_i is S_i.

Based on the 3σ principle, the 2018 version of MATLAB was used to find the displacement data corresponding to the outliers of the m-1 sample data obtained by Equation (1). If it is detected that S_{i} corresponding to $V(t_i)$ is an abnormal value, the replacement is performed according to Equation (2). After the replacement of outliers, the outliers are processed again according to the above method until there is no outlier in the data. S_m will be replaced with S_{m-1} if it is detected as an outlier. It is assumed here that S_1 obtained at the beginning is a normal value.

$$S_i = S_{i-1} + \frac{t_i - t_{i-1}}{t_{i+1} - t_{i-1}}(S_{i+1} - S_{i-1}), (i = 2, 3, 4, \cdots, m) \tag{2}$$

The corrected displacement curves can be obtained by the above method, and then used to obtain the longitudinal vibration curves. It is assumed that the displacement curve when drilling in the same rock formation is a straight line without considering vibration. Therefore, the longitudinal vibration can be obtained through Equation (3) during the actual drilling process.

$$L_i = S_i - Vt_i - a_0 \tag{3}$$

where L_i represents longitudinal vibration, cm, V indicates the penetration rate when drilling in the same strength rock formation, cm/s, a_0 is a constant term. V and a_0 can be obtained by linearly fitting the modified displacement curve.

The next step is to process the obtained sound pressure data. However, there are other noise disturbances in the data collected by the acoustic recorder. The relationship between the sound pressure level of each part can be described as Equation (4).

$$L_p = 10\lg\left(10^{0.1L_{p1}} + 10^{0.1L_{p2}}\right) \tag{4}$$

where L_{p1} represents noise sound pressure level, dBA, L_{p2} indicates Anchor rig sound pressure level, dBA, L_p recorded by the acoustic recorder donates mixed sound pressure level, dBA.

The data collected by the acoustic recorder during drilling and with different intervals are L_p and L_{p1}, respectively, which makes it difficult to separate L_{p2} from L_p during actual drilling. Therefore, after the above method was used for data anomaly detection and processing of L_{p1} and L_p, MATLAB was used to predict L_{p1} during the drilling period based on the neural network time series algorithm, and then L_{p2} during drilling was obtained by Equation (4).

3. Experimental Results

3.1. Sound Response Characteristics

The sound pressure level curves of a series of drill bits drilled in sandstone and sandy mudstone are shown in Figure 7, which indicates that there is no significant change in sound pressure levels when different drill bits are drilled in the same rock formation. However, the sound pressure levels when drilling in sandstone and sandy mudstone are concentrated between 110~120 dBA and 105~110 dBA, respectively. Therefore, the sound pressure level may be used as an important reference for rock formation interface identification when the strength of the roof rock layer changes.

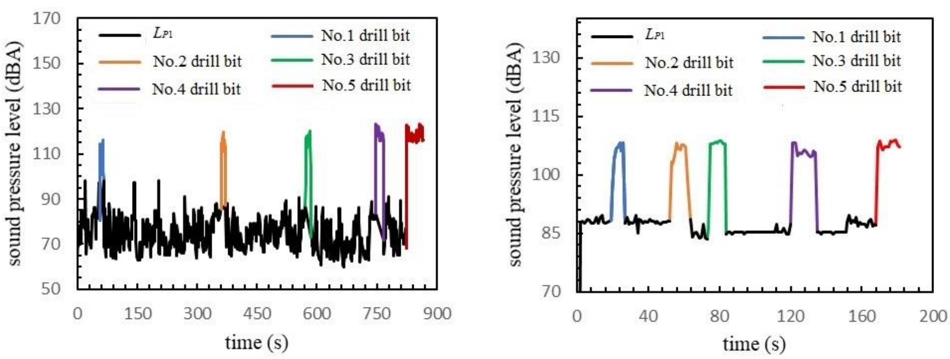

(**a**) sandstone (**b**) sandy mudstone

Figure 7. Sound curve of different bits in diameters when drilling.

3.2. Vibration Response Characteristics

Figure 8A–E,a–e show the displacement and longitudinal vibration curves of the drill bits 1 to 5 in sandstone and sandy mudstone, respectively. It can be concluded that the displacement curves are "upper step" and approximately a straight line with a constant amplitude in the same rock formation. Furthermore, the penetration rate gradually decreases as the diameter of the bit increases and the penetration rate in sandstone is smaller than in sandy mudstone under the same conditions. From the perspective of longitudinal vibration, and the longitudinal vibration amplitude of the 42 mm diameter drill bit is significantly larger. The longitudinal vibration amplitude when drilling in the sandstone is greater than that in the sandy mudstone. Compared with the new drill bit, both the penetration rate and the longitudinal vibration amplitude of the worn bit are reduced, and the penetration rate decreases significantly when drilling in the higher strength sandstone.

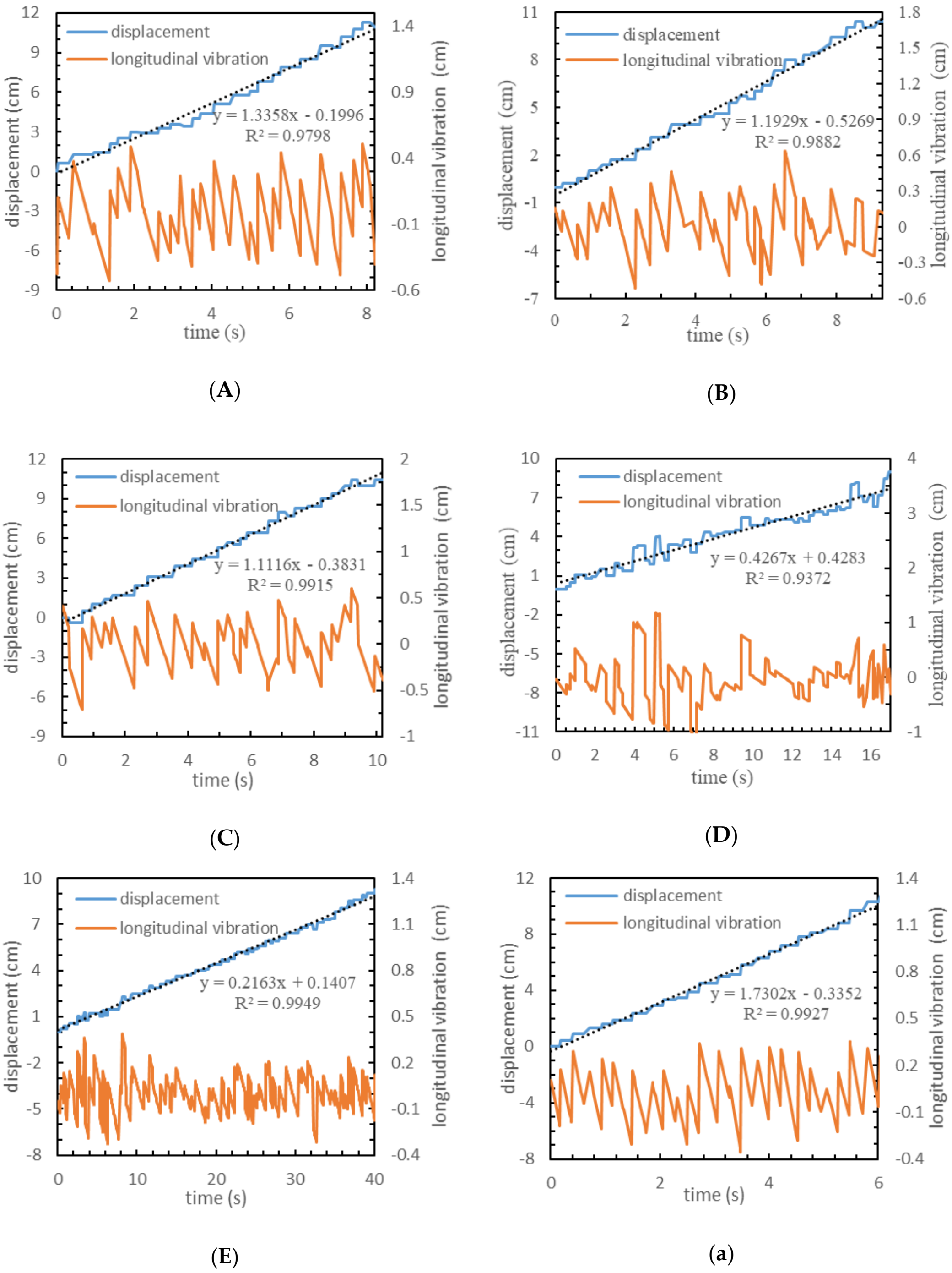

Figure 8. *Cont.*

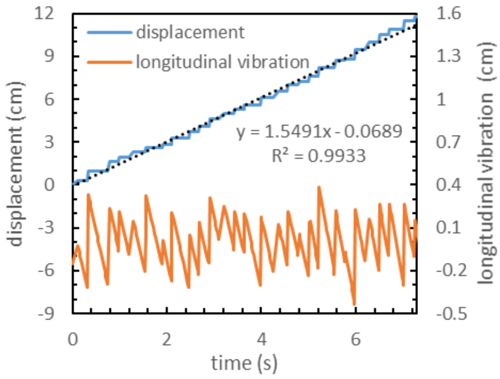

(**b**)

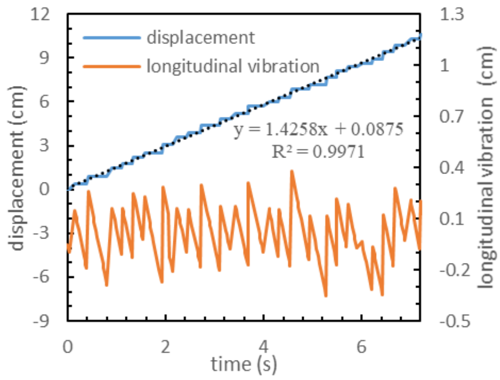

(**c**)

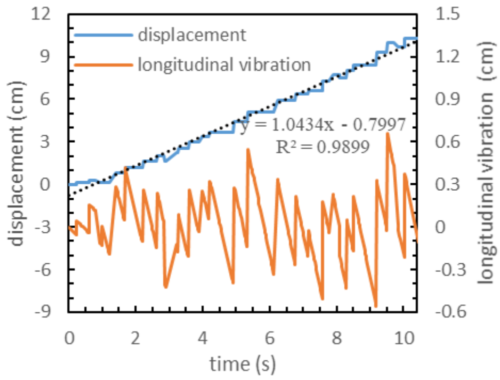

(**d**)

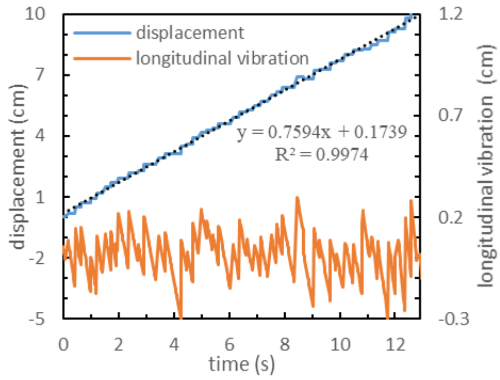

(**e**)

Figure 8. Displacement and longitudinal vibration curves of different bits. (**A**) The displacement and longitudinal vibration curves of the drill bit 1 in sandstone. (**B**) The displacement and longitudinal vibration curves of the drill bit 2 in sandstone. (**C**) The displacement and longitudinal vibration curves of the drill bit 3 in sandstone. (**D**) The displacement and longitudinal vibration curves of the drill bit 4 in sandstone. (**E**) The displacement and longitudinal vibration curves of the drill bit 5 in sandstone. (**a**) The displacement and longitudinal vibration curves of the drill bit 1 in sandy mudstone. (**b**) The displacement and longitudinal vibration curves of the drill bit 2 in sandy mudstone. (**c**) The displacement and longitudinal vibration curves of the drill bit 3 in sandy mudstone. (**d**) The displacement and longitudinal vibration curves of the drill bit 4 in sandy mudstone. (**e**) The displacement and longitudinal vibration curves of the drill bit 5 in sandy mudstone.

3.3. Distribution Characteristics of Cuttings Particles

Figure 9 indicates the cuttings screening results of sandstone borehole and sandy mudstone borehole.

0~0.074 mm 0.074~0.25 mm 0.25~0.5 mm 0.5~0.8 mm >0.8 mm

(**a**) sandstone

Figure 9. *Cont.*

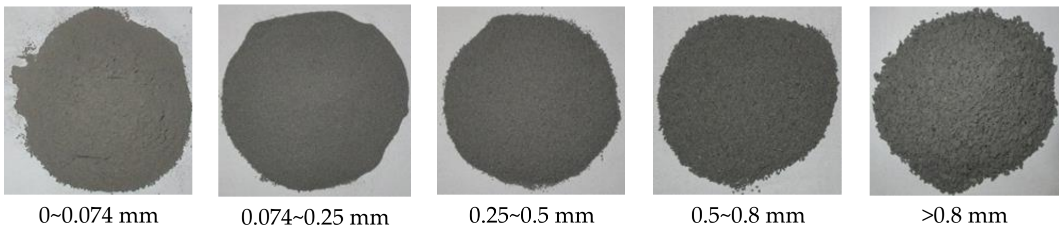

(**b**) sandy mudstone

Figure 9. Partial drilling cuttings screening results. (**a**) sandstone; (**b**) sandy mudstone

The percentage of different cuttings particles calculated by sifting the collected cuttings from each borehole is shown in Figure 10. Figure 10A–E,a–e represent the distribution of cuttings particles in sandstone and sandy mudstone, respectively.

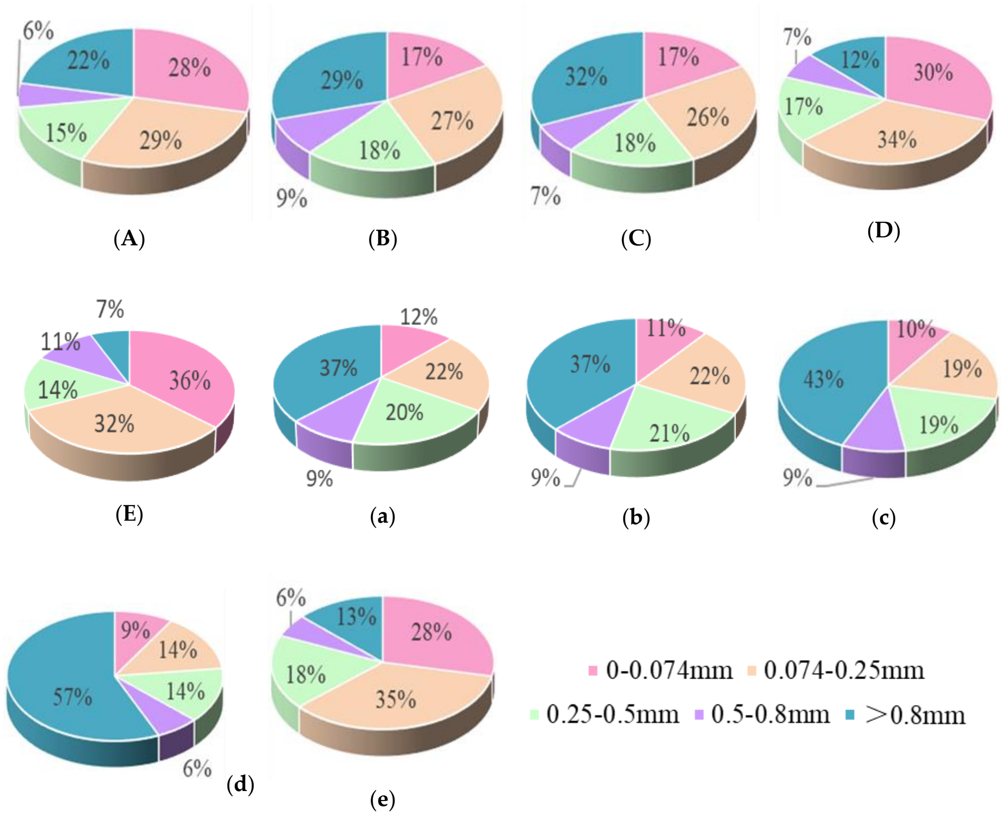

Figure 10. The pie chart of the cuttings particle's distribution. (**A**) The cuttings particle's distribution of drill bit 1 in sandstone. (**B**) The cuttings particle's distribution of drill bit 2 in sandstone. (**C**) The cuttings particle's distribution of drill bit 3 in sandstone. (**D**) The cuttings particle's distribution of drill bit 4 in sandstone. (**E**) The cuttings particle's distribution of drill bit 5 in sandstone. (**a**) The cuttings particle's distribution of drill bit 1 in sandy mudstone. (**b**) The cuttings particle's distribution of drill bit 2 in sandy mudstone. (**c**) The cuttings particle's distribution of drill bit 3 in sandy mudstone. (**d**) The cuttings particle's distribution of drill bit 4 in sandy mudstone. (**e**) The cuttings particle's distribution of drill bit 5 in sandy mudstone.

It can be found that the cuttings particle's size has an increasing trend when the bit diameter is changed from 28 mm to 30 mm during drilling in the sandstone, and the increasing trend is obviously slowing down when the bit diameter is changed from 30 mm to 32 mm. Additionally, the size of the cuttings for 0 mm to 0.074 mm increases to 30%, and exceeding 0.8 mm, the size decreases to 12% when the bit diameter is changed from 32 mm to 42 mm.

In the same manner, the percentage of cuttings larger than 0.8 mm increased from 37% to 57% when the drill diameter increased from 28 mm to 42 mm during drilling in the sandy mudstone. In short, the cuttings particle's size increases when the corresponding bit diameter increases.

Compared with sandy mudstone, the percentage of cuttings particles larger than 0.8 mm when drilling in sandstone is significantly smaller and smaller than 0.074 mm is significantly larger. In short, cuttings particles are larger when drilling in sandy mudstone.

Moreover, compared with the worn bit, the percentage of new bit cuttings larger than 0.8 mm is significantly larger (22% > 7%, 37% > 13%). The percentage of the cutting's diameter of the worn bit between 0.074 mm and 0.28 mm is significantly increased. In conclusion, compared with the worn bit, the cuttings particles of the new bit are larger when drilling in the rock, which is also the main reason for the high efficiency of the new bit.

3.4. Drilling Efficiency Analysis

Under the same drilling conditions, the drilling efficiency of different drill bits was evaluated by the rock-breaking volume per unit time, which is shown in Figure 11, after the trend line slope is regarded as the penetration rate. Based on the findings in the sandstone, the rock-breaking volume per unit time increases gradually when the diameter of the new drill bit increases from 28 mm to 32 mm, and the rock-breaking volume decreases significantly when the diameter increases to 42 mm. Likewise, in the sandy mudstone, the rock-breaking volume per unit time increases slowly when the diameter of the new drill bit increases from 28 to 32 mm, and the rock-breaking volume increases significantly when the diameter increases to 42 mm. Meanwhile, as compared to the new drill bit, the volume of rock-breaking per unit time of the worn bit is significantly reduced. Especially for the sandstone with higher strength, the reduction is more obvious.

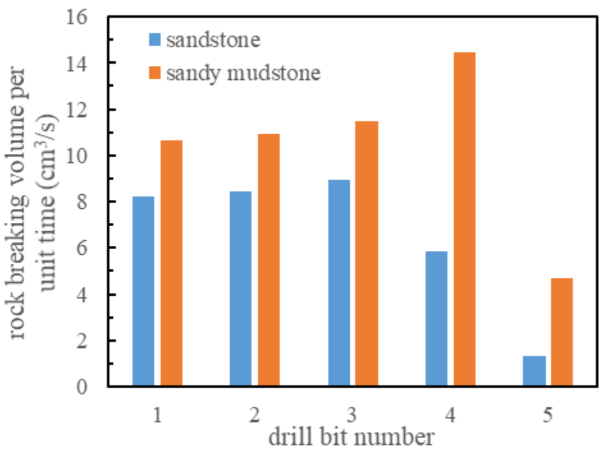

Figure 11. The rock-breaking volume per unit time for different bit diameters.

4. Discussion

The numerical simulation results of the two-wing PDC bit when drilling in rock strata with different strengths show that the higher the rock stratum strength, the lower the penetration rate, and the larger the fluctuation range of the penetration rate and the greater the lateral and longitudinal vibration frequency of the drill rod [16,21]. To some extent, the numerical simulation results support the experimental results in this paper. Additionally, Figure 12 shows another group of the cuttings particle's distribution, which is not shown in Figure 10 due to the overall structure of the article. Both holes were drilled under the same conditions using a No. 1 drill bit, and the distance from the No. 1 hole shown in Figure 5 is within 300 mm. The experimental results are basically consistent with those in Figure 10. Although there may be some errors in the data, the distribution characteristics of cuttings particles in the two rock formations with large differences in intensity are obviously different.

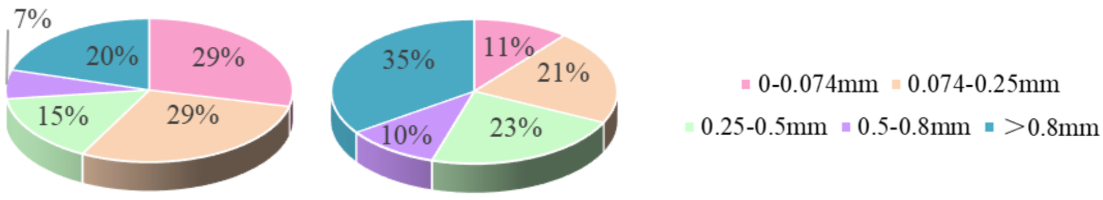

(**a**) sandstone (**b**) sandy mudstone

Figure 12. The pie chart of the cuttings particle's distribution.

Laboratory experiments and numerical simulations have found that more than 95% of the energy is used for torque work, and the percentage of torque work has an increasing trend as the rock strength increases [21,22]. However, the rock-breaking ability of the worn bit under the action of torque drops sharply compared to the axial thrust when drilling in the higher strength rock, which may be the reason why the penetration rate of No. 5 drill bit drops more significantly when drilling in the sandstone compared to the sandy mudstone.

Theoretically, the rock-breaking volume per unit time is equal when the rock of the same strength is drilled. However, as seen in Figure 11, the rock-breaking efficiency of the No. 4 drill bit and No. 5 drill bit is significantly reduced, which has a great correlation with the size distribution of the cutting particles. More energy is needed to break the rock into smaller cuttings particles than large cuttings particles.

Rock formation identification technology based on the characteristics of drilling response is relatively mature in the field of petroleum and geological exploration, while the research on the characteristics of drilling response of anchor drill bits (two-wing PDC drill bit) is relatively rare. Moreover, there are many more experiments to study the rock cutting process of PDC bits through numerical simulation than field experiments [23–26]. In this paper, field experiment data collection is realized, which provides a reference for peer field experiments and the development of detection while drilling equipment. In addition, the 3σ principle is used to process abnormal data, and the sound pressure and noise are separated using a time-series neural network, which provides an important reference for similar data processing.

The research finding expresses the following enlightenments:

1. Sound pressure level, penetration rate, longitudinal vibration, and the cuttings collection device shown in Figure 3 can be used to identify the interface and thickness of various formations.
2. A new method for bit wear and drilling efficiency evaluation can be established based on the distribution characteristics of drill cuttings.
3. Drilling efficiency can be improved by optimizing the bit structure so that the broken rock blocks flow out of the anchor holes as early as possible to avoid being broken into cuttings.
4. The drilling efficiency may be improved by optimizing the thrust and torque distribution ratio of the pneumatic bolt rig for different strength rock layers.

These drilling response characteristics are of great significance for further understanding of the rock-breaking mechanism of the two-wing PDC bit. However, these experimental holes have a smaller depth than the actual drilling depth. Consequently, the relationship between drilling depth and each drilling response characteristic will be studied in the field experiments.

5. Conclusions

In this paper, two-wing PDC bits of different diameters were used to drill in sandstone and sandy mudstone, and the sound pressure level, displacement, longitudinal vibration, and rock cuttings during the drilling process were analyzed and discussed. The experimental study yielded the following conclusions.

(1) Contrary to cuttings particles and the penetration rate, the sound pressure level and the longitudinal vibration are larger when drilling in the higher strength sandstone. Sound pressure level, penetration rate, longitudinal vibration, and the cuttings collection devices, shown in Figure 3, provide a reference for identifying the interface and thickness of various formations.

(2) The size of the cuttings particles has an increasing tendency as the drill diameter increases in the sandy mudstone. The cuttings particles are significantly smaller than the other three drill bits when the diameter of the 42 mm drill bit is drilled in the sandstone. Additionally, compared with the sandstone cuttings particles, the sandy mudstone cuttings particles are significantly larger. The following situations may exist under certain conditions, the higher the rock strength, the smaller the cuttings particles, and the lower the drilling efficiency.

(3) Compared to sandy mudstone, the decrease of drilling efficiency is more obvious when drilling in higher strength sandstone with the worn bit.

Author Contributions: Data curation, C.L.; Formal analysis, C.L., X.Z., and G.W.; Funding acquisition, X.Z.; Investigation, C.L.; Project administration, X.Z. and Z.L.; Software, C.L. and M.X.; Writing—original draft, C.L.; Writing—review and editing, C.L., X.Z., and G.W. All authors have read and agreed to the published version of the manuscript.

Funding: This research was funded by the National Natural Science Foundation of China (51574226), the Fundamental Research Funds for the Central Universities (2017CXNL01) and 2017 Special Project of Subject Frontiers Scientific Research in China University of Mining and Technology (2017XKQY047).

Acknowledgments: The authors are grateful to the staff at the Panzhihua Coal Mine and Wangjiazhai Coal Mine for their assistance during the field experiments.

Conflicts of Interest: The authors declare no conflict of interest.

Abbreviations

PDC	Polycrystalline Diamond Compact
UCS	Uniaxial Compressive Strength
t_i	Time corresponding to the i-th data
S_i	Displacement corresponding to the i-th data
V	Constant velocity when drilling in the same strength rock formation
$V(t_i)$	Penetration rate corresponding to t_i time
L_i	Longitudinal vibration
L_p	Mixed sound pressure level
L_{p1}	Noise sound pressure level
L_{p2}	Anchor rig sound pressure level
μ	Mean value of sample data
σ	Standard deviation of sample data

References

1. Ajibose, O.K.; Wiercigroch, M.; Akisanya, A.R. Experimental studies of the resultant contact forces in drillbit–rock interaction. *Int. J. Mech. Sci.* **2015**, *91*, 3–11. [CrossRef]
2. Yang, Y.X.; Zhang, C.L.; Lin, M.; Chen, L. Research on rock-breaking mechanism of cross-cutting PDC bit. *J. Pet. Sci. Eng.* **2018**, *161*, 657–666. [CrossRef]
3. Cai, C.; Wu, K.S.; Lian, D.; Yuan, X.H. Study of rock-breaking mechanism under single-tooth impact. *Rock. Soil. Mech.* **2015**, *36*, 1659–1666 and 1675. [CrossRef]

4. Yahiaoui, M.; Gerbaud, L.; Paris, J.Y.; Denape, J.; Dourfaye, A. A study on PDC drill bits quality. *Wear* **2013**, *298*, 32–41. [CrossRef]
5. Karasawa, H.; Ohno, T.; Miyazaki, K.; Eko, A. Experimental results on the effect of bit wear on torque response. *Int. J. Rock Mech. Min. Sci.* **2016**, *84*, 1–9. [CrossRef]
6. Botti, L.; Mora, C.; Antonucci, A.; Carty, P.; Barr, A.; Rempel, D. Carbide-tipped bit wear patterns and productivity with concrete drilling. *Wear* **2017**, *386*, 58–62. [CrossRef]
7. Wang, S.Y.; Sloan, S.W.; Liu, H.Y.; Tang, C.A. Numerical simulation of the rock fragmentation process induced by two drill bits subjected to static and dynamic (impact) loading. *Rock Mech. Rock Eng.* **2011**, *44*, 317–332. [CrossRef]
8. Cheng, Z.; Sheng, M.; Li, G.; Huang, Z.; Shi, H.; Dai, X.; Guo, Z. Cracks imaging in linear cutting tests with a PDC cutter: Characteristics and development sequence of cracks in the rock. *J. Pet. Sci. Eng.* **2019**, *179*, 1151–1158. [CrossRef]
9. Cheng, Z.; Sheng, M.; Li, G.; Huang, Z.; Wu, X.; Zhu, Z.; Yang, J. Imaging the formation process of cuttings: Characteristics of cuttings and mechanical specific energy in single PDC cutter tests. *J. Pet. Sci. Eng.* **2018**, *171*, 854–862. [CrossRef]
10. Wang, X.; Wang, Z.; Wang, D.; Chai, L. A novel method for measuring and analyzing the interaction between drill bit and rock. *Measurement* **2018**, *121*, 344–354. [CrossRef]
11. Miyazaki, K.; Ohno, T.; Karasawa, H.; Takakura, S.; Eko, A. Performance evaluation of polycrystalline diamond compact percussion bits through laboratory drilling tests. *Int. J. Rock Mech. Min. Sci.* **2016**, *87*, 1–7. [CrossRef]
12. Sun, R.; Ju, P.; Shi, Z. Simulation study of new directional drilling PDC bit used in coal mine. *Geosystem Eng.* **2017**, *20*, 142–148. [CrossRef]
13. Huang, K.; Ai, Z.; Yang, Y.; Xie, Z. The improved rock breaking efficiency of an annular-groove PDC bit. *J. Pet. Sci. Eng.* **2019**, *172*, 425–435. [CrossRef]
14. Cancan, L.; Xigui, Z.; Arifuggaman, A.; Mengbin, X. Measurement and analysis of penetration rate and vibration on a roof bolter for identification rock interface of roadway roof. *Energy Sources Part A Recovery Util. Environ. Eff.* **2019**. [CrossRef]
15. Li, W. Research on Theory and Method for Identification of Rock Mass Properties Based on Drilling Response. Available online: http://kreader.cnki.net/Kreader/CatalogViewPage.aspx?dbCode=cdmd&filename=1017132164.nh&tablename=CDFDLAST2017&compose=&first=1&uid=WEEvREcwSlJHSldRa1FhcTdWa2FjcW9xcjNWTUZ2TWtZTjdCS2JqMVRsND0=$9A4hF_YAuvQ5obgVAqNKPCYcEjKensW4IQMovwHtwkF4VYPoHbKxJw!! (accessed on 25 December 2019).
16. Liu, S.; Luo, Y.; Jia, H. Vibration mechanism and characteristics analysis of drill rod when drilling roof bolt hole. *J. China Univ. Min. Technol.* **2016**, *45*, 893–900. [CrossRef]
17. Gradl, C.; Eustes, A.W., III; Thonhauser, G. An analysis of noise characteristics of drill bits. *J. Energy Res. Technol.* **2008**, *134*, 681–687. [CrossRef]
18. Ma, Y.; Huang, Z.; Li, Q.; Zhou, Y.; Peng, S. Cutter layout optimization for reduction of lateral force on pdc bit using kriging and particle swarm optimization methods. *J. Pet. Sci. Eng.* **2018**, *163*, 359–370. [CrossRef]
19. Dougherty, P.S.M.; Pudjoprawoto, R.; Fred Higgs, C. Bit cutter-on-rock tribometry: Analyzing friction and rate-of-penetration for deep well drilling substrates. *Tribol. Int.* **2014**, *77*, 178–185. [CrossRef]
20. Qiu, P.H. *Introduction to Statistical Process Control*; Taylor & Francis Group: Boca Raton, FL, USA, 2014; pp. 104–105.
21. Liu, S.W.; Luo, Y.F.; Jia, H.S. Energy response characteristics of rock interface under drilling of roof anchorage borehole in coal roadway. *J. China Univ. Min. Technol.* **2018**, *47*, 88–96. [CrossRef]
22. Wang, Q.; Qin, Q.; Gao, S.; Li, S.C.; Gao, H.K.; He, M.C.; Jiang, B.; Zhang, C. Relationship between rock drilling parameters and rock uniaxial compressive strength based on energy analysis. *J. China Coal Soc.* **2018**, *43*, 1289–1295. [CrossRef]
23. Rojek, J.; Onate, E.; Labra, C.; Kargl, H. Discrete element simulation of rock cutting. *Int. J. Rock Mech. Min. Sci.* **2011**, *48*, 996–1010. [CrossRef]
24. Su, O.; Akcin, N.A. Numerical simulation of rock cutting using the discrete element method. *Int. J. Rock Mech. Min. Sci.* **2011**, *48*, 434–442. [CrossRef]

25. Li, X. Study on the Roof Drilling Characteristics Experiment of Anchorage Hole in Coal Roadway. Available online: http://kreader.cnki.net/Kreader/CatalogViewPage.aspx?dbCode=cdmd&filename=1016711111.nh&tablename=CMFD201602&compose=&first=1&uid=WEEvREcwSlJHSldRa1FhcTdWa2FjcW9xck9nSUVubEdzck9xSUYySHJGYz0=$9A4hF_YAuvQ5obgVAqNKPCYcEjKensW4IQMovwHtwkF4VYPoHbKxJw!! (accessed on 25 December 2019).
26. Liu, D. Research of the Dynamic Response Characteristics in the Drilling of Anchor Hole in the Roof of Roadway. Available online: http://kreader.cnki.net/Kreader/CatalogViewPage.aspx?dbCode=cdmd&filename=1015903273.nh&tablename=CMFD201701&compose=&first=1&uid=WEEvREcwSlJHSldRa1FhcTdWa2FjcW9xck9nSUVubEdzck9xSUYySHJGYz0=$9A4hF_YAuvQ5obgVAqNKPCYcEjKensW4IQMovwHtwkF4VYPoHbKxJw!! (accessed on 25 December 2019).